Two modes for dune orientation

Sylvain Courrech du Pont[1]*, Clément Narteau[2], and Xin Gao[2]

[1]Laboratoire Matière et Systèmes Complexes, Sorbonne Paris Cité, Université Paris Diderot, CNRS UMR 7057, 10 rue A. Domon et L. Duquet, 75205 Paris Cedex13, France

[2]Institut de Physique du Globe de Paris, Sorbonne Paris Cité, Université Paris Diderot, CNRS UMR 7154, 1 rue Jussieu, 75238 Paris Cedex 05, France

ABSTRACT

Earth's sand seas (dune fields) experience winds that blow with different strengths and from different directions in line with the seasons. In response, dune fields show a rich variety of shapes, from crescentic barchans to star and linear dunes. These dunes commonly exhibit complex and compound patterns with a range of length scales and various orientations, which up to now have remained difficult to relate to wind cycles. Here, we develop a model for dune orientation that explains the coexistence of bedforms with different alignments in multidirectional wind regimes. This model derives from subaqueous experiments, which show that a single bidirectional flow regime can lead to two different dune orientations depending on sediment availability, i.e., the erodibility of the bed. Sediment availability selects the overriding mechanism for the formation of dunes: increasing in height from the destabilization of a sand bed (with no restriction in sediment availability) or elongating in a finger on a nonerodible surface from a localized sand source. These mechanisms drive the dune orientation. Therefore, dune alignment maximizes dune orthogonality to sand fluxes in the bed instability mode, while dunes are aligned with the mean sand transport direction in the fingering mode. Applied to Earth's deserts, the model quantitatively predicts the orientation of rectilinear dunes and their superimposed patterns. This field study suggests that many linear dunes on Earth elongate from sources, and are simply aligned with the mean sand transport direction.

INTRODUCTION

Dunes in arid sand seas are usually classified into three groups, distinguished by the directional variability of winds (Pye and Tsoar, 1990). Where winds are unidirectional and sand is scarce, crescentic barchan dunes migrate on a non-erodible floor; as the amount of sand increases, barchans link into barchanoid and then transverse ridges, perpendicularly to the mean wind direction (Figs. 1A and 1F). Sand seas exposed to a wide, multidirectional wind regime show star dunes, characterized by a massive pyramidal morphology with multiple radiating arms (Pye and Tsoar, 1990; Zhang et al., 2012). Finally, for a moderate wind direction variability, typically a bimodal wind regime with an obtuse divergence angle between winds, linear dunes are observed (Figs. 1B and 1C). Because of seasonal climatic variations, linear dunes are the most common dunes on Earth (Lancaster, 1982). They are long, relatively straight, parallel ridges that have been recognized to extend in the resultant wind direction (Tsoar, 1983; Livingstone, 1988) and to migrate laterally (Rubin and Hunter, 1985; Bristow et al., 2000; Rubin et al., 2008). Blown by winds from either side, their crests are reversing and can be sinuous but sharp in cross section, so that linear dunes are also referred to as seif ("sword" in Arabic) dunes. This stands for simple linear dunes but they can also be wide ridges, up to 200 m high, with superim-
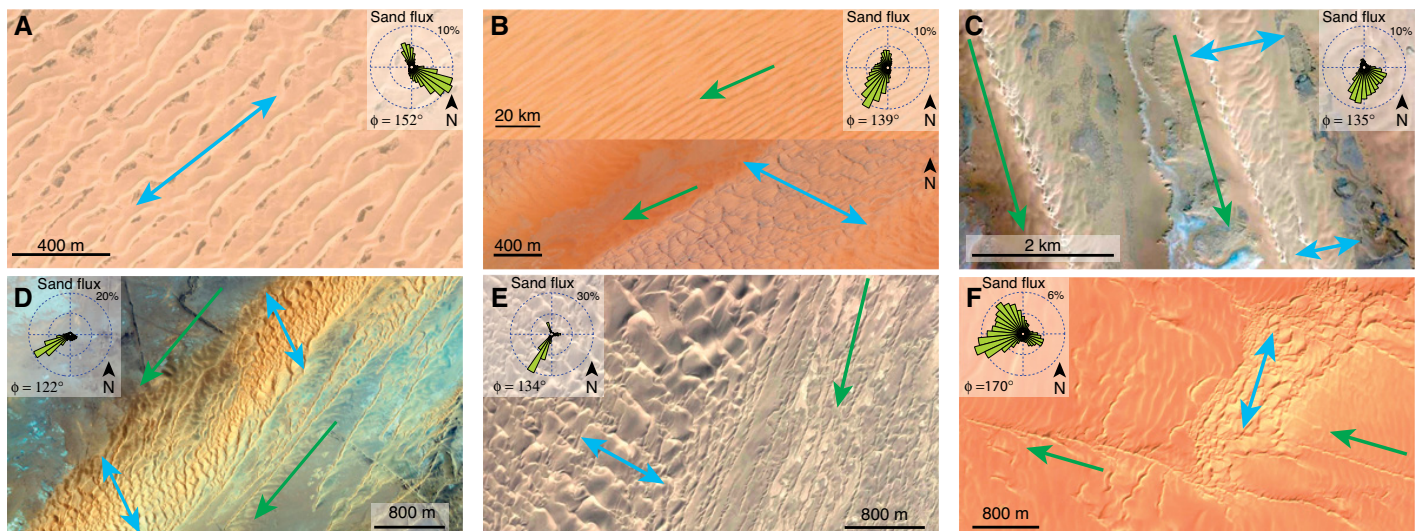

Figure 1. Two modes of dune orientation in sand seas. A: Oblique barchanoid ridges in Mu Us Desert (China, 38.8°N, 107.7°E). B: Linear dune field (top) and superimposed bedform (bottom) in Rub' al Khali (Saudi Arabia, 19.3°N, 48.5°E). C: Linear (seif) dunes with superimposed bedform in Great Sand Sea (Egypt, 26.15°N, 26.9°E). D: Linear dune with superimposed bedform in Erg Chech-Adrar (Mali, 23.6°N, 5.1°W). Note that coexistence of small active dunes of similar size with two different orientations cannot be ascribed to a temporal change of wind regime. E: Spatial transition between two orientations for dunes in Taklamakan Desert (China, 38.3°N, 86.7°E). The transition from bed-instability mode (west) to fingering mode (east) corresponds to an abrupt decrease in sand availability in the inter-dune areas. F: Compound transverse dunes in Ubari Desert (Libya, 26.8°N, 12.6°E) with defects that align in fingering mode and extend from sand patches. Each panel shows sand flux rose, divergence angle ϕ, and predicted dune orientations, with blue arrows for bed-instability mode and green arrows for fingering mode. Low-contrast bedforms seen in inter-dune areas in panels B, C, and F appear to be sand sheets (Pye and Tsoar, 1990; see Fig. DR27 [see footnote 1]). Pictures are from Google Earth™. See the Data Repository (see footnote 1) for more comparisons and details.

*E-mail: sylvain.courrech@univ-paris-diderot.fr.

posed dunes on their surface, which are usually oblique or transverse to the primary trend (Lancaster, 1982) (Fig. 1B).

Experiments on the formation of aeolian ripples (Rubin and Hunter, 1987), underwater dunes (Rubin and Ikeda, 1990; Reffet et al., 2010), and aeolian dunes in the field (Ping et al., 2014) within a bidirectional flow regime show that the bedform alignment maximizes the gross sand transport normal to the crest. Depending on the transport ratio and the divergence angle between winds, this leads to the formation of dunes that are transverse, oblique, or longitudinal with respect to the mean transport direction. Consequently, transverse dunes migrate, longitudinal dunes extend, and oblique dunes both migrate and extend. Using this concept, the orientation of dunes can be used as a proxy for wind regime (Lancaster et al., 2002; Bourke et al., 2010; Fenton et al., 2013; Telfer and Hesse, 2013). However, its application to aeolian dunes on Earth, using modern winds, reveals a clear mismatch for linear dunes (Lancaster et al., 2002; Lancaster, 2010). This discrepancy may be ascribed to the age of dunes that have been dated back to the Last Glacial Maximum (Lancaster et al., 2002). Wind regimes may have changed significantly since then. This seems to be supported by the difference observed between the primary (old) linear dune trend and the orientation of the smaller (modern) superimposed bedform.

Here we link all these observations with a model that explains the coexistence of different bedform orientations within a single wind regime. Thus, we predict the orientation of primary dunes and of their superimposed patterns using modern winds. The model derives from the experimental observation that a single flow regime can shape dunes with two distinct orientations, depending on the sand supply.

METHODS

We experimentally study the formation of dunes subjected to a bidirectional flow regime underwater, where the characteristic sizes (centimetric) and times are downscaled (Reffet et al., 2010). The bedform, made of 90-μm-diameter ceramic beads, lies on a 70-cm-wide plate, which translates from one end to the other of a 2-m-long water tank. The translation is fast (30 cm/s) in order to generate transport in one direction, and slow (2 cm/s) to prevent grain motion in the other. This sequence, a blow, simulates a unidirectional flow over the bedform. The plate alternately rotates by an angle θ (−θ) every 2 blows ($N \times 2$ blows), to change the apparent direction of the flow. We vary the divergence angle θ and the transport ratio N (ratio between alternate numbers of blows) between the main and the second flow directions. We perform experiments with three different sand-supply conditions: (1) an initial 2-mm-thick flat sand bed with no additional sand supply, (2) an initial flat sand bed with systematic sand supply where the plate becomes visible, and (3) an initial 1 g conical pile at a point with periodic sand supply (typically 0.4 g every 20 blows) at the same point. The bedform evolution is followed through time with top-view images and three-dimensional profiles. Dune orientation is measured by autocorrelation.

In our model, the prevailing dune growth mechanism selects dune orientation. As a result, orientations maximize dune growth rate when dunes increase in height or correspond to the mean sand flux direction when dunes extend from a sediment source. These quantities are derived from sand fluxes over dunes.

To predict the orientation of dunes in the field, we collect wind velocities and direction from the ERA-Interim assimilation project (Dee et al., 2011). This general circulation model provides wind data at 10 m above ground since A.D. 1979, with a 0.75° horizontal resolution and a 6 h time resolution. We calculate the corresponding sand fluxes for sand grains of 180 μm using the model of Ungar and Haff (1987). The resulting predicted orientations are not very sensitive to transport laws and parameters (Table DR1 in the GSA Data Repository[1]). Orientation of dunes is measured by autocorrelation from Google Earth™ images (Fig. DR15 in the Data Repository). See the Data Repository for full details.

UNDERWATER EXPERIMENTS

Figure 2 shows the morphodynamics of dunes for different sand supply conditions but within the same bidirectional flow regime, characterized by a divergence angle θ = 130° and a transport ratio $N = 5$.

Starting from a flat sand bed with a limited depth, a bedform instability develops roughly perpendicular to the dominant flow direction (Fig. 2A). This orientation is maintained while dunes increase in height and wavelength, until the non-erodible surface of the table is reached (Figs. 2D–2F). Without sand supply, the bed instability can no longer develop. As a result, these crest-reversing but migrating dunes become unstable and break. Instead of simply breaking into barchans, as observed when the flow is unidirectional (Reffet et al., 2010; Parteli et al., 2011), they reconnect through extending fingers (Movie DR1 in the Data Repository). In response to this change in sand availability, the dune field switches orientation to a dune trend that is more parallel to the dominant flow direction. While

sand availability selects only the dune morphology under a unidirectional flow (i.e., barchans or transverse dunes), this experimental result demonstrates that it can also select the dune orientation in a multidirectional flow regime.

Indeed, starting from the same initial conditions but regularly adding sand to the inter-dune areas to maintain the erodibility of the bed, the development of the bed instability is preserved. Dunes keep increasing in height, with a stationary orientation almost perpendicular to the prevailing flow direction (Figs. 2B and 2D–2F; Movie DR2). This is consistent with previous experimental studies performed with a bed completely covered with sand (Rubin and Hunter, 1987; Rubin and Ikeda, 1990; Reffet et al. 2010; Ping et al., 2014).

When sand supply is restricted to a fixed point source, we observe a straight extending finger with a sharp crest and a reversing avalanche face (Fig. 2C; Movie DR3). This finger dune is reminiscent of an asymmetric barchan with an elongating arm (Bagnold, 1941; Parteli et al., 2009; Reffet et al., 2010; Bourke et al., 2010; Taniguchi et al., 2012). Its very growth mode makes it aligned with the mean sand transport direction. However, note that it is significantly different (by 24°) from the resultant flow direction (Fig. 2C). This is the signature of the interaction between dune shape and sediment transport, which has to be taken into account to accurately predict dune orientation.

Depending on sand supply, the same flow regime leads to two dune orientations, here differing by 49°. These results are generic to asymmetric flow conditions once θ exceeds 90° (see the Data Repository). Sand supply determines the preponderant mechanism in the dune development, which drives the dune orientation. Having identified the two mechanisms (i.e., increasing height with the development of the bed instability, or extension away from a sand source along the sand transport direction), we can now develop a complete model for dune orientation.

MODEL FOR DUNE ORIENTATION

Let us consider a field of linear dunes of orientation, α, with $\vec{i}$ in the standard basis $(\vec{i}, \vec{j})$, shaped by an arbitrary wind cycle of duration T. Instantaneous flux magnitude Q_0 and direction ψ depend on time t. A positive topography makes the wind accelerate, so that the sand flux over a dune depends on the dune shape experienced by the wind (Jackson and Hunt, 1975). To the first order in dune aspect ratio, H/W (height over width), the maximum saturated sand flux is:

$$\vec{Q}_s(t) = Q_0(t)\left(1 + \beta \frac{H}{W}\left|\sin[\psi(t) - \alpha]\right|\right)\left[\cos\psi(t)\,\vec{i} + \sin\psi(t)\,\vec{j}\right], \quad (1)$$

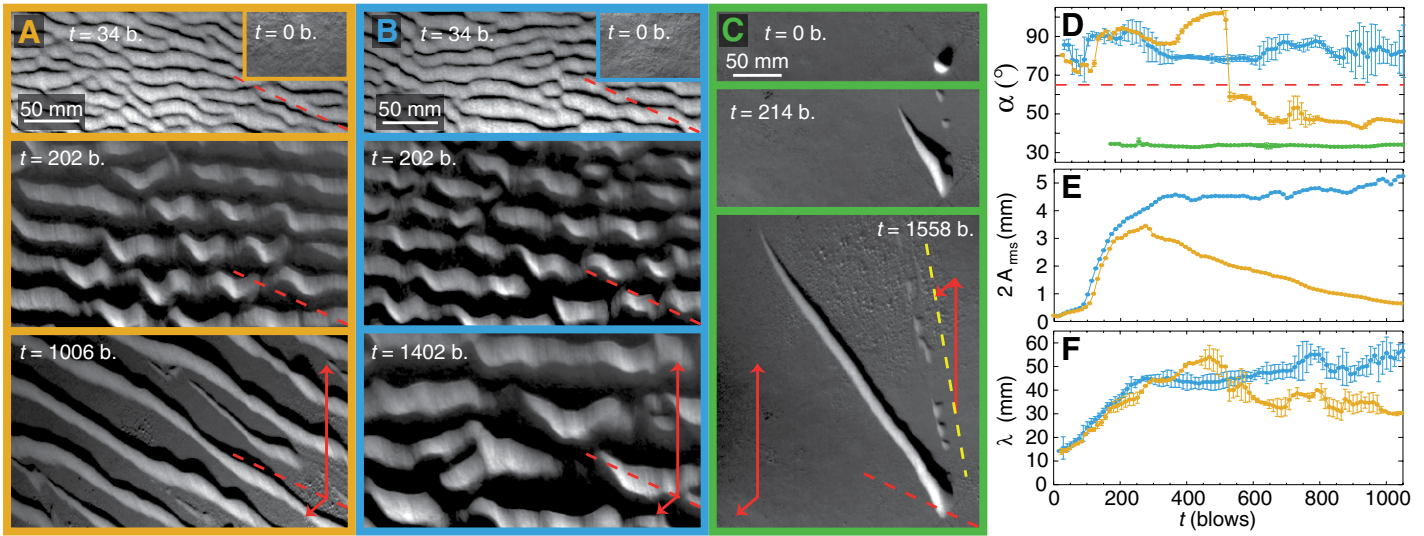where Q_0 is the value of the saturated sand flux over a flat sand bed, β is a dimensionless

Figure 2. Two modes of dune orientation in experiments. Flow regime is the same for all experiments: divergence angle θ = 130° and transport ratio N = 5. Pictures capture dunes after the prevailing flow sequence (b.—blows). Red vectors show transport vectors of the two consecutive flows. Red dashed line is the bisector of the angle between the two flow directions. A: Dunes developing from a flat sand bed with a limited depth. B: Evolution of a dune field from flat sand bed with infinite sand availability. C: Finger dune extending on a non-erodible ground from a fixed sand source. Note that the same orientation is observed for an array of finger dunes, extending from the breaking of a large isolated transverse dune (see the Data Repository [see footnote 1]). Extension direction is different from resultant drift direction (yellow dashed line). The tray of small barchans also emitted from the source moves along the resultant drift direction. D–F: Orientation, α, amplitude, 2 A$_{rms}$, and wavelength, λ, of dunes over time, t. Time is measured in numbers of blows. A flow period counts 12 blows. Yellow, blue, and green points show results for dunes developing from sand bed with limited depth (A), from sand bed with infinite sediment availability (B), and from fixed sand source (C), respectively. Amplitude was not measured for dunes developing from a fixed sand source (D) and no wavelength can be associated to a single dune. Red dashed line (half value of the divergence angle θ) delimits the two modes of orientation. For the limited sand availability experiment, note the sharp reorientation of the dune field when it stops increasing in height (t of ~520 blows), once the inter-dune is free of sand.

coefficient that accounts for the wind velocity increase (Jackson and Hunt, 1975), and $(H / W)\left|\sin[\psi - \alpha]\right|$ is the dune aspect ratio experienced by the wind, which blows in the direction $\left[\cos\psi\ \vec{i}\ +\ \sin\psi\ \vec{j}\right]$. In a multidirectional wind regime, the wind velocity increase introduces a dependency between the direction of the mean sand flux and the dune orientation α.

With no limitation in sand availability, dunes result from the development of the bed instability (Fig. 2B). Thus, they increase in height with a selected orientation, which should correspond to the highest growth rate of dunes. The law of mass conservation reads $\vec{\nabla}.\vec{Q} = -\partial h / \partial t$, where the sand flux Q and bedform height h are functions of space and time. If the structure does not propagate, ∂h/∂t represents the growth rate of the structure. The sediment flux over the dune typically varies from its maximum saturated value to zero $\left(\left\|\vec{Q}_s(t)\right\|$; Equation 1) on a characteristic length that scales with the dune width in the wind direction $W /\left|\sin\left[\psi(t) - \alpha\right]\right|$. Thus, if the dune is large enough to keep a constant overall shape over the wind cycle, the growth rate σ averaged over T scales as:

$$\sigma \propto \frac{1}{T\ HW} \int_T \left\|\vec{Q}_s(t)\right\| \left|\sin\left[\psi(t) - \alpha\right]\right|\ dt. \quad (2)$$

Growth rate σ is a function of α, and the preferred orientation, α_I, is the one for which the growth rate is maximum, such that dσ/dα = 0.

As defined, the resulting dune orientation yields to the maximum gross transport normal to the bedform trend, as proposed by Rubin and Hunter (1987) with a wind velocity increase correction.

In contrast, when dunes form on a non-erodible floor from fixed sediment sources, they extend in the direction α_F of the mean sand flux $\langle \vec{Q} \rangle$ (Fig. 2C), which is given by the integration of instantaneous fluxes over T (Equation 1). Then, the finger dune orientation α_F is such that: $\tan\alpha_F = \langle \vec{Q}(\alpha_F) \rangle \,.\, \vec{j} / \langle \vec{Q}(\alpha_F) \rangle \,.\, \vec{i}$. The very existence of a finger dune aligned in the mean flux direction may be surprising. Indeed, such a dune cannot develop under a unidirectional wind. However, in a multimodal wind regime, the finger dune pointing in the mean flux direction is blown on either side by winds, which can build and sustain the dune (see the Data Repository).

In Earth sand seas, linear dunes are typically observed for a multidirectional wind regime with an obtuse divergence angle. For such a wind regime, the two predicted orientations α_I and α_F are equal when the wind regime is symmetric, e.g., a bidirectional wind regime with a transport ratio equal to 1. Dunes align along the bisector of the angle between the two flow directions. The two modes differ more and more as a wind direction prevails over the others: dunes in the bed-instability mode tend to be perpendicular to the prevailing wind, whereas dunes in the fingering mode tend to align with it. See the

Data Repository for analytical solutions of α_I and α_F for bidirectional wind regimes and their comparison to experimental results.

FIELD STUDY

Figure 1 compares field observations in sand seas of the Northern Hemisphere to our model predictions. Predicted orientations are computed from sand flux distributions corresponding to wind data of the past 30 yr with a topography parameter βH/W (Equation 1) set to 1, which is a typical reported value (Walker et al., 2009; see the Data Repository). As expected, where there is no sediment in the inter-dune areas, one observes linear dunes in the fingering mode (Figs. 1B–1D and 1E, right). In zones with no limitation in sand availability, dunes are in the bed-instability mode (Figs. 1A and 1E, left). This mode is observed for the main bedform in regions where sand accumulates, but also for the superimposed structures on large linear finger dunes (Figs. 1B–1D). Indeed, these giant dunes represent an erodible floor where the bed instability develops. The two modes of orientation are generic, and can coexist as superimposed patterns or where there is an abrupt spatial transition in sand availability (Fig. 1E). Although the coexistence of dunes with different orientations could result from a change in wind regimes, it finds here a simple and consistent explanation.

Our model is quantitatively compared to all field data in Figure 3. It accurately predicts dune orientation within 5°, not only for small dunes (~30 m wide) but also for larger and older dunes (~1 km wide). This suggests that the 30 yr data of modern winds used to predict dune orientation provide an accurate picture of the wind regimes that built these sand seas in the past.
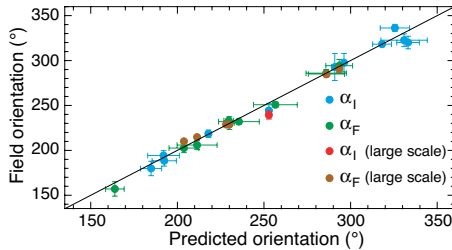

Figure 3. Predicted versus observed dune orientation for the bed instability mode (α_I) and the fingering mode (α_F) in sand seas of Northern Hemisphere. Orientations are measured counterclockwise with respect to east for 11 regions in the Sahara, Rub' al Khali, Taklamakan, and Mu Us deserts. Aside from their orientation, dune fields commonly exhibit two different length scales for dune width or wavelength: a small one (~30 m) and a large one (~1 km). We measure their corresponding orientations separately. Vertical and horizontal error bars stand for standard deviations in measurements and model sensitivity to transport onset velocity, respectively. See the Data Repository (see footnote 1) for a detailed record of field data.

CONCLUSION

Our experiments and field study show that a single multidirectional wind regime can shape dunes with two distinct orientations. The orientation depends on the mechanism that prevails for the formation of dunes, which is determined by sand availability. Thus, with no limitation in sand availability, when dunes develop from the destabilization of a sand bed and build up with sediment coming from the inter-dune, one observes dunes whose orientation maximizes the growth rate (or the gross transport normal to the crest; Rubin and Hunter, 1987). Dunes within this bed-instability mode are usually oblique to the mean sand transport direction, and extend and shift sideways, so that they morphologically look like barchanoid ridges. In contrast, when sand is scarce, typically when dunes develop on a non-erodible floor with a sediment supply restricted to a localized source, dunes are aligned with the mean sediment transport direction. Within this fingering mode, dunes mainly extend and morphologically look like seif dunes or large straight ridges with oblique superimposed patterns. Although the range of wind regimes under which finger dunes can develop is still to be determined, our field studies show that many dunes on Earth sand seas are aligned with the mean sand transport direction (Figs. 1 and 3). Such longitudinal alignment could correspond to the bed-instability mode, but it would then result from symmetric wind regimes. This is not what is observed in the field. These dunes are in the fingering mode, which suggests that they extend away from geomorphologic sand sources (e.g., coastal or fluvial-alluvial systems). Indeed, the spreading nature of the fingering mode is likely to produce vast dune fields, with hundreds-of-kilometers-long and parallel linear dunes as observed on Earth sand seas.

REFERENCES CITED

Bagnold, R.A., 1941, The Physics of Blown Sand and Desert Dunes: London, Chapman and Hall, 265 p.

Bourke, M.C., Lancaster, N., Fenton, L.K., Parteli, E.J.R., Zimbelman, J.R., and Radebaugh, J., 2010, Extraterrestrial dunes: An introduction to the special issue on planetary dune systems: Geomorphology, v. 121, p. 1–14, doi:10.1016/j.geomorph.2010.04.007.

Bristow, C., Bailey, S., and Lancaster, N., 2000, The sedimentary structure of linear sand dunes: Nature, v. 406, p. 56–59, doi:10.1038/35017536.

Dee, D., et al., 2011, The ERA-Interim reanalysis: Configuration and performance of the data assimilation system: Quarterly Journal of the Royal Meteorological Society, v. 137, p. 553–597, doi:10.1002/qj.828.

Fenton, L.K., Michaels, T.I., and Beyer, R.A., 2013, Inverse maximum gross bedform-normal transport 1: How to determine a dune-constructing wind regime using only imagery: Icarus, v. 230, p. 5–14, doi:10.1016/j.icarus.2013.04.001.

Jackson, P., and Hunt, J., 1975, Turbulent wind flow over a low hill: Quarterly Journal of the Royal Meteorological Society, v. 101, p. 929–955, doi:10.1002/qj.49710143015.

Lancaster, N., 1982, Linear dunes: Progress in Physical Geography, v. 6, p. 475–504, doi:10.1177/030913338200600401.

Lancaster, N., 2010, Assessing dune-forming winds on planetary surfaces: Application of the gross bed form normal concept: Second International Planetary Dunes Workshop, Alamosa, Colorado, 18–21 May 2010: LPI Contribution No. 1552, p. 39–40.

Lancaster, N., Kocurek, G., Singhvi, A., Pandey, V., Deynoux, M., Ghienne, J.F., and Lô, K., 2002, Late Pleistocene and Holocene dune activity and wind regimes in the western Sahara Desert of Mauritania: Geology, v. 30, p. 991–994, doi:10.1130/0091-7613(2002)030<0991:LPAHDA>2.0.CO;2.

Livingstone, I., 1988, New models for the formation of linear sand dunes: Geography (Sheffield, England), v. 73, p. 105–115.

Parteli, E., Duràn, O., Tsoar, H., Schwämmle, V., and Herrmann, H., 2009, Dune formation under bimodal winds: Proceedings of the National Academy of Sciences of the United States of America, v. 106, p. 22,085–22,089, doi:10.1073/pnas.0808646106.

Parteli, E., Andrade, J., and Herrmann, H., 2011, Transverse instability of dunes: Physical Review Letters, v. 107, 188001, doi:10.1103/PhysRevLett.107.188001.

Ping, L., Narteau, C., Dong, Z., Zhang, Z., and Courrech du Pont, S., 2014, Emergence of oblique dunes in a landscape-scale experiment: Nature Geoscience, v. 7, p. 99–103, doi:110.1038/ngeo2047.

Pye, K., and Tsoar, H., 1990, Aeolian Sand and Sand Dunes: London, Unwin Hyman, 458 p.

Reffet, E., Courrech du Pont, S., Hersen, P., and Douady, S., 2010, Formation and stability of transverse and longitudinal sand dunes: Geology, v. 38, p. 491–494, doi:10.1130/G30894.1.

Rubin, D.M., and Hunter, R.E., 1985, Why deposits of longitudinal dunes are rarely recognized in the geologic record: Sedimentology, v. 32, p. 147–157, doi:10.1111/j.1365-3091.1985.tb00498.x.

Rubin, D.M., and Hunter, R.E., 1987, Bedform alignment in directionally varying flows: Science, v. 237, p. 276–278, doi:10.1126/science.237.4812.276.

Rubin, D.M., and Ikeda, H., 1990, Flume experiments on the alignment of transverse, oblique, and longitudinal dunes in directionally varying flows: Sedimentology, v. 37, p. 673–684, doi:10.1111/j.1365-3091.1990.tb00628.x.

Rubin, D.M., Tsoar, H., and Blumberg, D.G., 2008, A second look at western Sinai seif dunes and their lateral migration: Geomorphology, v. 93, p. 335–342, doi:10.1016/j.geomorph.2007.03.004.

Taniguchi, K., Endo, N., and Sekiguchi, H., 2012, The effect of periodic changes in wind direction on the deformation and morphology of isolated sand dunes based on flume experiments and field data from the western Sahara: Geomorphology, v. 179, p. 286–299, doi:10.1016/j.geomorph.2012.08.019.

Telfer, M., and Hesse, P., 2013, Palaeoenvironmental reconstructions from linear dune fields: Recent progress, current challenges and future directions: Quaternary Science Reviews, v. 78, p. 1–21, doi:10.1016/j.quascirev.2013.07.007.

Tsoar, H., 1983, Dynamic processes acting on a longitudinal (seif) sand dune: Sedimentology, v. 30, p. 567–578, doi:10.1111/j.1365-3091.1983.tb00694.x.

Ungar, J.E., and Haff, P.K., 1987, Steady state saltation in air: Sedimentology, v. 34, p. 289–299, doi:10.1111/j.1365-3091.1987.tb00778.x.

Walker, I., Hesp, P., Davidson-Arnott, R., Bauer, B., Namikas, S., and Ollerhead, J., 2009, Response of three-dimensional flow to variations in the angle of incident wind and profile form of dunes: Greenwich Dunes, Prince Edward Island, Canada: Geomorphology, v. 105, p. 127–138, doi:10.1016/j.geomorph.2007.12.019.

Zhang, D., Narteau, C., Rozier, O., and Courrech du Pont, S., 2012, Morphology and dynamics of star dunes from numerical modelling: Nature Geoscience, v. 5, p. 463–467, doi:10.1038/ngeo1503.